THE JOURNAL OF BIOLOGICAL CHEMISTRY VOL. 286, NO. 18, pp. 16504–16515, May 6, 2011

Alternative Mitochondrial Electron Transfer as a Novel Strategy for Neuroprotection*

Received for publication, December 15, 2010, and in revised form, March 2, 2011 Published, JBC Papers in Press, March 18, 2011, DOI 10.1074/jbc.M110.208447

Yi Wen[‡], Wenjun Li[‡], Ethan C. Poteet[‡], Luokun Xie[‡], Cong Tan[‡], Liang-Jun Yan[‡], Xiaohua Ju[‡], Ran Liu[‡], Hai Qian[‡], Marian A. Marvin[§], Matthew S. Goldberg[§¶], Hua She[‖], Zixu Mao[‖**], James W. Simpkins[‡], and Shao-Hua Yang[‡1]**

*From the [‡]Department of Pharmacology and Neuroscience, Institute for Alzheimer's Disease and Aging Research, University of North Texas Health Science Center, Fort Worth, Texas 76107, the Departments of [§]Neurology and [¶]Psychiatry, University of Texas Southwestern Medical Center, Dallas, Texas 75390, and the Departments of [‖]Pharmacology and **Neurology, Emory University, Atlanta, Georgia 30322*

Neuroprotective strategies, including free radical scavengers, ion channel modulators, and anti-inflammatory agents, have been extensively explored in the last 2 decades for the treatment of neurological diseases. Unfortunately, none of the neuroprotectants has been proved effective in clinical trails. In the current study, we demonstrated that methylene blue (MB) functions as an alternative electron carrier, which accepts electrons from NADH and transfers them to cytochrome *c* and bypasses complex I/III blockage. A *de novo* synthesized MB derivative, with the redox center disabled by *N*-acetylation, had no effect on mitochondrial complex activities. MB increases cellular oxygen consumption rates and reduces anaerobic glycolysis in cultured neuronal cells. MB is protective against various insults *in vitro* at low nanomolar concentrations. Our data indicate that MB has a unique mechanism and is fundamentally different from traditional antioxidants. We examined the effects of MB in two animal models of neurological diseases. MB dramatically attenuates behavioral, neurochemical, and neuropathological impairment in a Parkinson disease model. Rotenone caused severe dopamine depletion in the striatum, which was almost completely rescued by MB. MB rescued the effects of rotenone on mitochondrial complex I-III inhibition and free radical overproduction. Rotenone induced a severe loss of nigral dopaminergic neurons, which was dramatically attenuated by MB. In addition, MB significantly reduced cerebral ischemia reperfusion damage in a transient focal cerebral ischemia model. The present study indicates that rerouting mitochondrial electron transfer by MB or similar molecules provides a novel strategy for neuroprotection against both chronic and acute neurological diseases involving mitochondrial dysfunction.

Mitochondria are the powerhouses and the major source of free radicals in almost all cells. Mitochondrial dysfunction is implicated in numerous neuropathological diseases, including Parkinson disease (PD)[2] (1, 2), Alzheimer disease (AD) (3), and stroke (4). Other than ATP production, mitochondria participate in diverse cell signaling events and are essential organelles for cell survival. The oxidative phosphorylation machinery is composed of five complexes (complexes I–V). From Krebs cycle intermediates (NADH and $FADH_2$), electrons feed into complex I or II and are transferred to complex III and then to complex IV and finally to the oxygen molecules. Energy released during the electron transfer is utilized to actively pump out proton from the mitochondrial matrix to the intermembrane space, generating the electrochemical gradient of proton across the inner membrane, which is ultimately utilized by complex V to produce ATP (5). However, a small portion of electrons leaking from the electron transport chain (ETC), mostly at complex I and complex III, react with the oxygen molecule and yield superoxide anion, which can be converted into other reactive oxygen species (ROS). When ROS production overwhelms the endogenous antioxidant systems, they can potentially damage various cellular components, including proteins, lipids, and nucleic acids. ROS is implicated in aging and various pathological processes and has been proposed as the key culprit for many neurodegenerative diseases. Thus, mitochondrial targeting strategies, such as free radical scavengers, mitochondrial signaling regulation, and ETC component supplementation, have been extensively studied (6, 7). Disappointingly, none of these neuroprotective strategies has been proven successful in any neurological diseases in clinical trials (8, 9).

Methylene blue (MB) is a heterocyclic aromatic compound that has many biological and medical applications. It is an FDA-approved drug for methemoglobinemia and an antidote to cyanide poisoning. Previous publications have suggested that MB improves mitochondrial function (10, 11). In the present study, we demonstrate that MB functions as an alternative electron carrier that efficiently shuttles electrons between NADH and

* This work was supported, in whole or in part, by National Institutes of Health Grants R01NS054687 (to S.-H. Y.), R01NS054651 (to S.-H. Y.), P01AG22550 (to J. W. S.), P01AG10485 (to J. W. S.), ES015317 (to Z. M.), AG023695 (to Z. M.), and NS048254 (to Z. M.). This work was also supported by Alzheimer's Association Grant NIRG57698 (to Y. W.) and Texas Garvey Foundation (to Y. W.).

[1] To whom correspondence should be addressed: Dept. of Pharmacology and Neuroscience University of North Texas Health Science Center, 3500 Camp Bowie Blvd., Fort Worth, TX 76107-2699. Tel.: 817-735-2250; Fax: 817-735-2091; E-mail: shaohua.yang@unthsc.edu.

[2] The abbreviations used are: PD, Parkinson disease; AD, Alzheimer disease; MB, methylene blue; MBH2, leucomethylene blue; ETC, electron transport chain; ROS, reactive oxygen species; ICA, internal carotid artery; DCFH2, 2,7-dichlorofluorescin; FCCP, carbonyl cyanide-*p*-trifluoromethoxyphenylhydrazone; OCR, oxygen consumption rate; ECAR, extracellular acidification rate; TH, tyrosine hydroxylase; cyt *c*, cytochrome *c*; Veh/Sal, vehicle/saline; ROT/Sal, rotenone/saline; ROT/MB, rotenone/MB; ICA, internal carotid artery; ANOVA, analysis of variance; DOPAC, 3,4-dihydroxyphenylacetic acid; VTA, ventral tegmental area; SNC, substantia nigra pars compacta.

cytochrome *c* (cyt *c*). This process reroutes electron transfer upon complex I and III inhibition, reduces electron leakage, and attenuates ROS overproduction. MB is protective in a rotenone-induced animal model of Parkinsonism and an animal model of ischemic stroke induced by middle cerebral artery occlusion.

EXPERIMENTAL PROCEDURES

Animals and Reagents—Male Sprague-Dawley rats (230–250 g; approximately 10 weeks old) (Charles River, Wilmington, MA) were housed individually with controlled temperature (22–25 °C) and humidity (55%). A 12-h light-dark cycle was maintained, with lights on between 7 a.m. and 7 p.m. All housing and procedures were performed in accordance with the guidelines of the Institutional Care and Use Committee of the National Research Council and were approved by the University of North Texas Health Science Center Animal Care and Use Committee.

Mitochondrial Isolation and Mitochondrial Respiration Chain Activity Assays—Fresh rat heart was removed and placed in ice-cold mitochondrial isolation buffer containing 210 mM mannitol, 70 mM sucrose, 5 mM HEPES, and 1 mM EDTA, pH 7. The heart was homogenized immediately, and the mitochondrial fraction was isolated by differential centrifugation as described previously (12). Mitochondria were stored at −80 °C until subsequent analysis.

All mitochondrial activity assays were performed according to previous publications with minimal modifications for complex I (13), complex I-III, complex II, complex III, and complex II-III (12). All assays used a similar master mix that contained potassium phosphate, pH 7.4 (50 mM), BSA (2.5 mg/ml), $MgCl_2$ (5 mM), KCN (2 mM), and various inhibitors or substrates, including rotenone (6 μM), antimycin A (2 μM), NADH (150 μM), coenzyme Q1 (60 μM), cyt *c* (50 μM), succinate (8 mM), and decyl-ubiquinol (100 μM). Complex I activity was monitored by adding NADH to the mix with or without rotenone/antimycin A. The final data were normalized to blank values at time 0. The reaction was monitored in a kinetic spectrophotometer at 340 nm. Complex I activity was measured in arbitrary units and normalized to control levels for statistical analysis. Isolated mitochondria equivalent to 40–200 μg of mitochondrial protein was used for each assay, except for assays with inhibitors, when higher levels of mitochondria (3–5-fold) were used to ensure that inhibition was distinguishable. Final data were normalized to control levels. For complex I-III activity, the reaction was initiated with the addition of NADH, cyt *c* was used as final substrate, and its reduction was monitored at 550 nm. For assay of complex II-III activity, succinate was added instead of NADH, and the electron transfer to cyt *c* was performed according to a previous publication (10). To test whether the electrons from the reduced form of MB (MBH_2) can be transferred to cyt *c* in mitochondrial lysate, we added 10 μM 2,7-dichlorofluorescin diacetate (DCFH2; Invitrogen) to the reaction system. Free radicals convert non-fluorescent DCFH2 to highly fluorescent 2,7-dichlorofluorescin (DCF) (excitation, 488 nm; emission, 530 nm). In the presence of cyt c, which accepts electrons from MBH_2, conversion of DCFH2 to DCF is decreased.

Cell Viability Assay—HT-22 cells (gift from Dr. David Schubert, Salk Institute, San Diego, CA) were plated at 4,000 cells/well in 96-well plates and cultured overnight. Then cells were treated with vehicle (DMSO), rotenone (2–8 μM), antimycin A (1–10 μg/ml), or glucose oxidase (2–10 milliunits) in the presence or absence of various concentrations of MB for 24 h. At the end of the 24 h, the medium was removed, and the plates were rinsed with PBS and incubated with 10 μM calcein-AM (Invitrogen) in PBS for 20 min. Fluorescence was determined using a TECAN M200 microplate reader (San Jose, CA) with an excitation/emission set at 485/530 nm. Cell culture wells treated with bleach before rinsing were used as a blank.

Intracellular ATP Assay—HT-22 cells were plated in 96 wells at 5000 cells/well and cultured overnight. Vehicle or increasing concentrations of MB were added to the culture medium (n = 6–8) and incubated for 4 h. The ATP determination was performed with an ATP determination kit (Invitrogen). Carbonyl cyanide-*p*-trifluoromethoxyphenylhydrazone (FCCP) and potassium cyanide (KCN) were used as control for inhibition. A standard curve was performed in the same assay plate.

Seahorse XF-24 Metabolic Flux Analysis—HT22 cells were plated at 8000 cells/well and cultured on Seahorse XF-24 plates. Cells were grown in previously described medium and environments for 24 h. On the day of metabolic flux analysis, cells were changed to unbuffered DMEM (DMEM base medium supplemented with 25 mM glucose, 10 mM sodium pyruvate, 31 mM NaCl, 2 mM glutamine, pH 7.4) and incubated at 37 °C in a non-CO_2 incubator for 1 h. All medium and injection reagents were adjusted to pH 7.4 on the day of assay. Four base-line measurements of oxygen consumption rate (OCR) and extracellular acidification rate (ECAR) were taken before sequential injection of mitochondrial inhibitors. Specific readings indicated by the *arrows* were taken after each addition of mitochondrial inhibitor before injection of the subsequent inhibitors. The mitochondrial inhibitors used were oligomycin (10 μM), FCCP (1 μM), and rotenone (5 μM). OCR and ECAR were automatically calculated and recorded by the Seahorse XF-24 software. After the assays, plates were saved, and protein readings were measured for each well to confirm equal cell numbers/well. The percentage of change compared with the basal rates was calculated as the value of change divided by the average value of base-line readings.

Mitochondrial Superoxide and Cellular ROS Analysis—Mitochondrial specific superoxide and cellular ROS were measured with specific fluorescent probes. Briefly, HT-22 cells were treated with vehicle or 2 μM rotenone, with or without 100 ng/ml MB for 4 h. The cells were dissociated and then incubated in prewarmed PBS containing 0.5% BSA and H2*DCFDA* (Cellular ROS) or MitoSox (mitochondrial superoxide) for 15 min at 37 °C, followed by washing with PBS. The cells were then resuspended in supplemented RPMI 1640 for further incubation. The cells were analyzed with an FITC channel (Cellular ROS) or R-Phycoerythrin (PE) channel (MitoSox) using a BD™ LSRII flow cytometer.

Effect of MB on a Rotenone Model of PD—Rats were assigned to three groups. Control animals received vehicle infusion and daily saline injection (Veh/Sal; n = 6–8); a second group received rotenone infusion at a dose of 5 mg/kg/day and daily

saline injection (ROT/Sal; $n = 8–11$); and the third group received rotenone infusion (5 mg/kg/day) and MB injection at a dose of 500 μg/kg/day (ROT/MB; $n = 8–10$). Vehicle or rotenone was infused via Alzet osmotic minipumps that were filled with vehicle or rotenone dissolved in vehicle (equal volumes of dimethyl sulfoxide and polyethylene glycol). Pumps containing vehicle or rotenone were sterilized with UV irradiation and implanted subcutaneously in the back. Intraperitoneal injections were administered with normal saline or MB (500 μg/kg/day), diluted in normal saline to 500 μl of final volume. Rats were sacrificed on day 8 at 4 h after the last dose of MB or saline treatment.

Accelerating Rotarod Performance—The accelerating rotarod (Omnitech Electronics, Columbus, OH) measures running coordination and motor performance. The rotor consisted of a nylon cylinder with a 7-cm diameter mounted horizontally 35.5 cm above a padded surface. On a given trial, the rats were placed on the cylinder, the cylinder was rotated, and a timer switch was simultaneously activated. Acceleration continued from 0 to a maximum of 44 rpm until animals were unable to stay on top of the rotating rod and fell to the padded surface. Animals were removed at 90 s if they did not fall. When the rat landed on the surface, a photosensitive switch was tripped and the timer stopped. Rats were subjected to this test at 2 sessions/day, 3 trials/session, for seven sessions. A 20-min resting period was given between each trial. Animals were given at least a 2-h break time between sessions each day. Retention times on the rotating treadmill were recorded and plotted for analysis.

Neurological Assessment—Neurological assessment was performed by three evaluators blind to treatment conditions. The evaluators were initially trained until they produced consistent scores when evaluating rats in these tests. Subsequently, experimental subjects were randomized and presented to the evaluators individually. For each session, which consisted of three trials, an individual evaluator scored a rat in only one trial; thus, the final score for a session for each animal was the average score of the three evaluators. The categories included tremor, locomotion, bradykinesia, hypokinesia, posture, and gross motor skills. The details for the scoring systems were adapted from previous publications in various animal models, including 1-methyl-4-phenyl-1,2,3,6-tetrahydropyridine (MPTP) and 6-hyroxydopamine (6-OHDA) lesions (14, 15). The categories included the following: tremor (0, absent; 1, occasional or barely detectable; 2, frequent or easily detectable; 3, continuous or intense, while active or at rest); locomotion (0, uses all four limbs smoothly and symmetrically; 1, walks slowly, noticeable limp; 2, walks very slowly and with effort; 3, unable to ambulate); bradykinesia (0, quick, precise movements; 1, mild slowing of movements (normal for aged); 2, slow deliberate movements with marked impairment initiating movements; 3, no movements); hypokinesia (0, moves freely, alert, responsive; 1, reduced activity, moves less frequently (without provocation); 2, minimal activity, moves with provocation; 3, akinetic (essentially no movements); posture (0, normal posture, able to stand freely; 1, reduced posture (normal for aged), stands with limbs apart; 2, stooped posture, hunched, legs bent, often leans on cage walls; 3, unable to maintain posture, recumbent); and gross motor skills (0, able to retrieve small objects accurately; 1, reduced ability to retrieve small objects; 2, great difficulties in retrieving small objects; 3, unable to retrieve objects).

Catalepsy Measurement—Catalepsy was measured by a standard bar test and grid test adapted from a previous publication (16). For the bar test, the rats were placed with both front paws grasping a horizontal bar that was 9 cm above the surface. The time each animal took to remove one paw from the bar was manually measured by a stopwatch. The grid test involved placing the rats on a vertical wire grid (25.5 cm wide and 44 cm high with a space of 1 cm between each wire), and catalepsy was determined by the length of time the animals maintained all four paws on the grid using a stopwatch. The maximum descent latency was set at 300 s for the bar test and 60 s for the grid test.

Gait Analysis for Stride Length—For gait analysis, the fore and hind paws of each rat were painted with blue and red dye, respectively, and the animals were allowed to walk across an absorbent paper-covered straight alley runway (150 cm long, 20 cm wide, opaque walls 20 cm tall) into a dark compartment. Before the test, animals were put in the dark compartment for 2 min to habituate to the environment, and three pretraining runs were conducted for all rats. Three trials were conducted to obtain clear footprints for each animal. Prolonged stop or turning backward in the runway was considered a failed trial. The distances between individual steps were analyzed by two independent blinded observers. The average of the left and right stride distance for each animal was used for statistical analysis.

Tissue Collection—After completion of neurological assessments and behavioral tests, rats were killed on the 8th day of rotenone infusion under anesthesia induced by xylazine (20 mg/kg, intraperitoneally) and ketamine (100 mg/kg, intraperitoneally). All osmotic pumps were checked for the residual liquid to ensure proper drug delivery. The brains were harvested. One hemisphere was fixed by 4% paraformaldehyde in phosphate buffer for 48 h until processing for sectioning. The other hemisphere was snap-frozen in liquid nitrogen and kept at −80 °C until extraction for biochemical analysis. Striata dissected from a separate set of animals were used for analysis of monoamines by HPLC.

Transient Cerebral Ischemia—10-week-old male Sprague-Dawley rats (Charles River) were used. Transient cerebral ischemia was induced by an intraluminal filament middle cerebral artery occlusion model. Briefly, the internal carotid artery (ICA) was exposed, and a 3–0 monofilament nylon suture was introduced into the ICA lumen through a puncture and gently advanced to the distal ICA until proper resistance was felt. After 1 h, the suture was withdrawn for reperfusion, and the distal ICA was cauterized. At 24 h after reperfusion, the animals were sacrificed, and the brains were harvested. The brains were sectioned at 3, 5, 7, 9, 11, 13, and 15 mm posterior to the olfactory bulb. Each slice was incubated for 30 min in 2% 2,3,5-triphenyltetrazolium chloride in physiological saline and then fixed in 10% formalin. The stained slices were digitally photographed for measurement of ischemic lesion volume (Image-Pro Plus 4.1).

HPLC Analysis of Monoamines and Metabolites—For monoamine and metabolite measurement, striatum tissue was dissected from each hemisphere, weighed, and stored at −80 °C. For HPLC analysis, tissue samples were sonicated in 9 volumes

of 0.1 M perchloric acid containing 0.2 mM sodium metabisulfite and centrifuged at 15,000 rpm for 20 min at 4 °C in a bench top centrifuge to clear debris. Five μl of cleared supernatant was injected onto a C18 HPLC column and separated by isocratic elution at a flow rate of 0.6 ml/min with MD-TM mobile phase (ESA Inc., Chelmsford, MA). Neurotransmitter monoamines and metabolites were detected using an ESA CoulArray electrochemical detector with a model 5014B cell set to a potential of +220 mV. Peak areas were compared with a standard curve of external standards to calculate quantities of dopamine and metabolites per mg of tissue.

Immunohistochemistry—Rat hemispheres were sequentially incubated in 10, 20, and 30% sucrose overnight. The brains were then frozen in OCT (optimal cutting temperature) compound (VWR, San Francisco, CA) and sectioned in the coronal plane with a cryostat to produce 20-μm floating sections. For single immunohistochemistry studies, 20-μm sections were blocked with 5% normal goat serum and incubated in primary antibodies at 4 °C overnight. Sections were then immunostained with Picture Plus immunohistochemistry kits (Invitrogen). 3,3′-Diaminobenzidine tetrachloride was used to visualize the sections. The primary antibodies used include a monoclonal mouse antibody against tyrosine hydroxylase (TH) (1:500) (Millipore, Billerica, MA), a monoclonal anti-ubiquitin (1:800) (Millipore, Billerica, MA), and a monoclonal anti-α-synuclein (1:100) (Santa Cruz Biotechnology, Inc., Santa Cruz, CA). For fluoro-jade B staining, paraformaldehyde-fixed brain sections from brains in each group were stained according to the manufacturer's protocol (Millipore). The slides were first immersed in 1% NaOH in 80% alcohol for 5 min, followed by washing for 2 min in 70% alcohol and 2 min in distilled water. The slides were then transferred to a solution of 0.06% potassium permanganate for 10 min to ensure consistent background suppression between sections. The slides were then stained with 0.0004% fluoro-jade B solution for 20 min. Double labeling for TH and fluoro-jade B was achieved by immunofluorescence. Sections were initially stained with fluoro-jade B and then incubated with antibodies against TH for 1 h at room temperature, and Alexa 594-conjugated goat anti-mouse IgG was used to detect TH-positive cells. For controls, primary antibodies were omitted. Double stained sections were examined with conventional fluorescence microscopy, and images were captured on a Zeiss microscope linked to an image analysis system with selective filter sets to visualize FITC, rhodamine, and DAPI separately. 3,3′-Diaminobenzidine tetrachloride-immunostained sections were visualized with a bright field microscope, and images were collected with a color digital camera.

Total ROS Assay—Frozen brain tissue was placed in 10-fold volume/weight ice-cold PBS containing a protease inhibitor mixture (EMD Bioscience, Gibbstown, NJ) and homogenized rapidly with a Polytron power homogenizer. An aliquot was ultracentrifuged at 50,000 × *g* for 30 min. Supernatant was removed and analyzed for total ROS content using the fluorescence probe DCFH2. DCFH2 was dissolved in absolute ethanol, diluted with PBS (pH 7.4) to 125 μM, and added to sample brain extracts at a final concentration of 25 μM followed by incubation at 37 °C for 10 min. Fluorescence intensity was measured using a fluorometer (TECAN M200 microplate reader San Jose, CA) at an excitation/emission wavelength set of 485/530 nm. Data were presented as relative fluorescent intensity or percentage of control. DCFH2 without brain extracts was used as a blank and was consistently less than 1% of final fluorescence units.

Statistical Analysis—The data for mitochondrial complex activity with MB alone, animal body weight, dopamine/5-HT levels, and ROS *in vivo* were analyzed with one-way ANOVA; mitochondrial I-III activity assay with inhibitors, complex II-III assay with inhibitors, and cell viability assays were analyzed by two-way ANOVA (treatment group with concentration); and rotarod assay and neurological assessment were analyzed by three-way ANOVA (group, session/category, and performance). When a significant difference was detected by ANOVA, a *post hoc* Tukey's test was performed to identify a specific difference between groups. Values were expressed as means ± S.E. Between two indicated samples, Student's *t*-tests were used to acquire a *p* value. A *p* value of <0.05 was used to indicate statistical significance: *, $p < 0.05$; **, $p < 0.01$; ***, $p < 0.001$.

RESULTS

MB Increases Cellular Oxygen Consumption Rate and Reduces Anaerobic Glycolysis—MB has been previously reported to improve mitochondrial functions. In our initial experiments, we used a Seahorse cellular bioenergetic analyzer to examine the effects of MB on mitochondrial respiration and cellular glycolysis in transformed hippocampal HT-22 cells. Oligomycin (complex V inhibitor), FCCP (uncoupler), and rotenone (complex I inhibitor) were sequentially applied to determine the action of MB on the ETC. MB rapidly increased OCR despite all treatments (Fig. 1*A*). With 2 h of incubation, MB dose-dependently increased OCR from 264 ± 10 pmol/min with vehicle treatment to 594 ± 19 pmol/min with 10 μg/ml MB treatment (Fig. 1*B*) and reduced ECAR from 44 ± 4 mpH/min with vehicle treatment to 9 ± 3 mpH/min with 10 μg/ml MB treatment (Fig. 1*C*). In addition, MB dose-dependently attenuated rotenone-induced OCR inhibition (Fig. 1*D*). We determined the effect of MB on ATP production (Fig. 1*E*). Four h of MB treatment significantly increased cellular ATP levels in the HT-22 cells, which peaked at 1 ng/ml (3.34 nM). We used two control compounds: a potent oxidative phosphorylation uncoupler, FCCP, and a complex IV inhibitor, KCN. FCCP increases OCR, whereas KCN reduces OCR. However, both compounds significantly reduce intracellular ATP levels.

MB Directly Improves ETC I-III Activity and Protects against Complex I and III Inhibition—We analyzed the effects of MB on the overall activity of mitochondrial ETC complex I-III in extracted mitochondria. MB dose-dependently enhanced mitochondrial complex I-III activity, as evidenced by the enhanced electrons transfer from NADH to cyt *c*. An up to 9-fold increase of complex I-III activity was detected in the presence of increasing doses of MB (0.1–1 μg/ml) (Fig. 2, *A* and *B*). As a proof of concept for the mechanism, we modified MB with *N*-acetylation. This acetylation blocked the redox capacity of MB and completely eliminated the action of MB on complex I-III (Fig. 2, *B* and *C*). Similar assays were performed in the presence of a specific complex I inhibitor (rotenone) (Fig. 2*D*) and a specific complex III inhibitor (antimycin A) (Fig. 2*E*). A 90

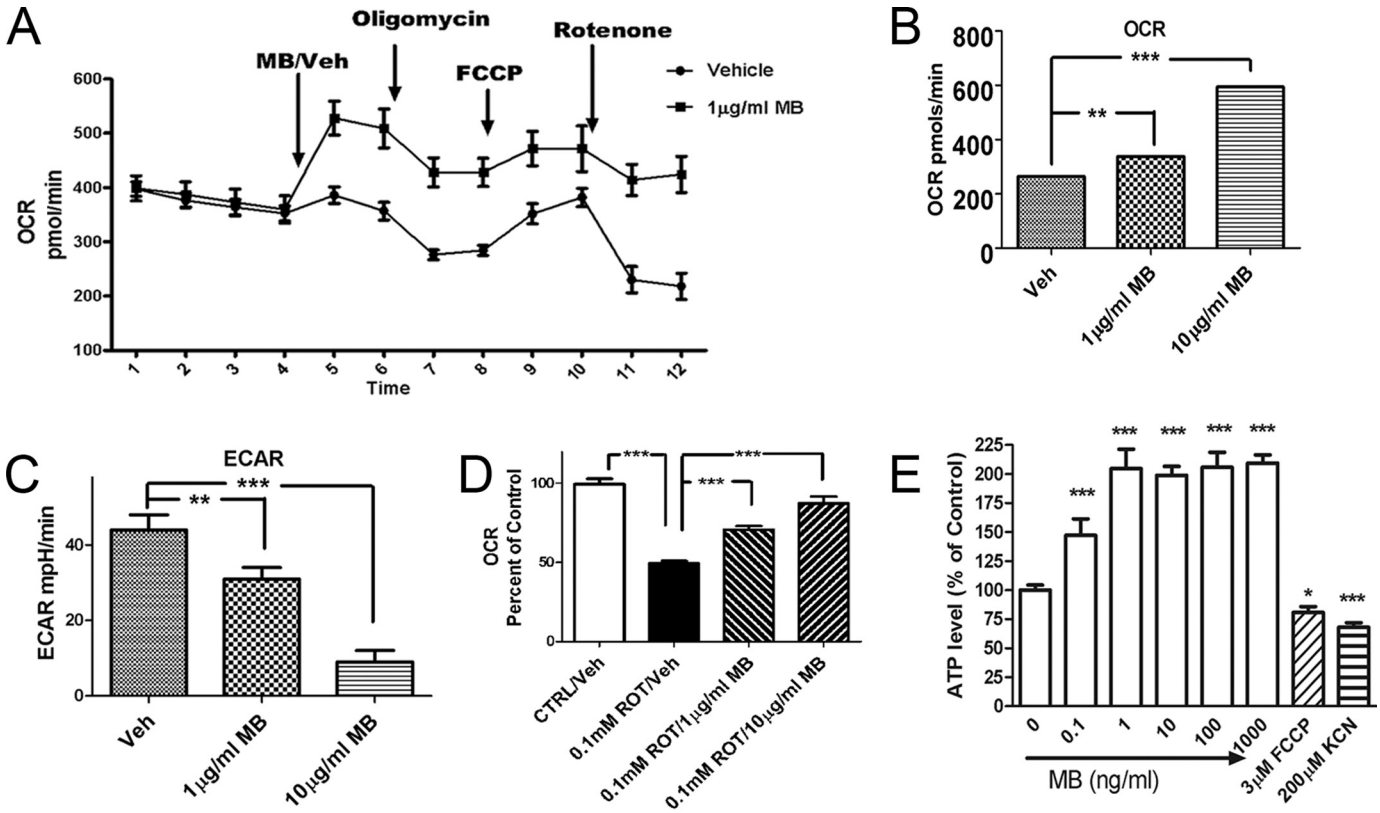

FIGURE 1. **MB improves mitochondrial respiration and reduces anaerobic glycolysis.** *A*, effects of MB on cellular oxygen consumption in HT-22 cells. Cellular oxygen consumption was monitored with sequential injection of MB/vehicle, oligomycin, FCCP, and rotenone. The vehicle- and MB-treated groups had a significant difference in OCR at all time points ($n = 5$). *B–D*, OCR (mitochondrial respiration) and ECAR were monitored with similar sequential treatment in *A* after 4-h MB/vehicle incubation at the indicated concentration. MB induced a significant dose-dependent increase in OCR (*B*), a dose-dependent decrease in ECAR (*C*), and a dose-dependent attenuation of rotenone-induced OCR inhibition (*D*) ($n = 5$). *E*, effects of MB on cellular ATP levels. Shown is a representative assay of intracellular ATP level in HT22 cells treated with the indicated concentration of MB. *, $p < 0.05$; ***, $p < 0.001$. *Error bars*, S.E.

and 70% inhibition of complex I-III activity was induced by rotenone and antimycin A, respectively. MB treatment dose-dependently prevented the inhibitory action of rotenone and antimycin A. Specifically, 1 μg/ml MB increased I-III activity to 118.1 $\pm$ 6.4% of control in the presence of rotenone (Fig. 2*D*). MB (1 μg/ml) increased such activity to 674 $\pm$ 99% of the control level in the presence of antimycin A (Fig. 2*E*). On the other hand, MB had no significant effects on complex II-III activity, for which 80% of activity was inhibited by antimycin A (Fig. 2*F*). These data demonstrate that MB is actively involved in the electron transfer process in mitochondria between complex I and complex III.

MB Forms a Redox Cycle between NADH and Cytochrome c That Reroutes Electrons between Complex I and III—We further examined the effects of MB on individual mitochondrial complex I, II, and III activities. MB had no significant effect on complex II or complex III activity alone (data not shown). However, we found that MB was a direct substrate of NADH dehydrogenase in mitochondrial complex I. In a typical complex I activity assay, coenzyme Q1, an endogenous substrate for complex I, was used to receive the electrons from NADH. This enzymatic reaction was very sensitive to rotenone (above 95% inhibition). Our results indicate that MB can act as an independent substrate to accept the electrons from NADH and convert MB to MBH_2 without the involvement of other physiological intermediates, such as coenzyme Q1 (*CoQ1*; Fig. 3, *A* and *C*). Such activity is relatively insensitive to rotenone inhibition (26.7% at maximum rotenone concentrations). We also observed that electrons from MBH_2 can be further delivered to cyt *c* in a competitive manner (Fig. 3, *B* and *D*). In this experimental setup, DCFH2 was used as a probe to monitor electron transfer. Without cyt *c*, MB facilitated the electron transfer from NADH and enhanced the oxidation of the DCFH2 probe. In the presence of cyt *c*, MBH_2 transferred electrons to cyt *c* instead of DCFH2, leading to a decrease in DCFH2 oxidation. The addition of cyt *c* significantly decreased oxidation of the DCFH2 in a dose-dependent manner (Fig. 3, *B–D*), suggesting that the reduced form of MB (MBH_2) is able to deliver the electrons to cyt *c* in mitochondria.

MB Protects against Rotenone- and Antimycin A-induced Cytotoxicity and Decreases Mitochondrial Superoxide and Cellular ROS Production under Stress—We examined the effects of MB treatments on mitochondrial oxidative phosphorylation inhibition in HT-22 cells. A significant protective action of MB against complex I inhibition (rotenone) toxicity was seen at all rotenone concentrations examined. At the highest rotenone concentration (8 μM), cell survival increased from 25.4 $\pm$ 1.6% with vehicle co-treatment to 60.5 $\pm$ 4.5% survival with 100 ng/ml MB co-treatment (Fig. 4*A*). Significant protection was also found with MB against complex III inhibitor (antimycin A) at various concentrations. At the highest antimycin A concentrations tested (25 μg/ml), 19.4 $\pm$ 3.0% cells survived without

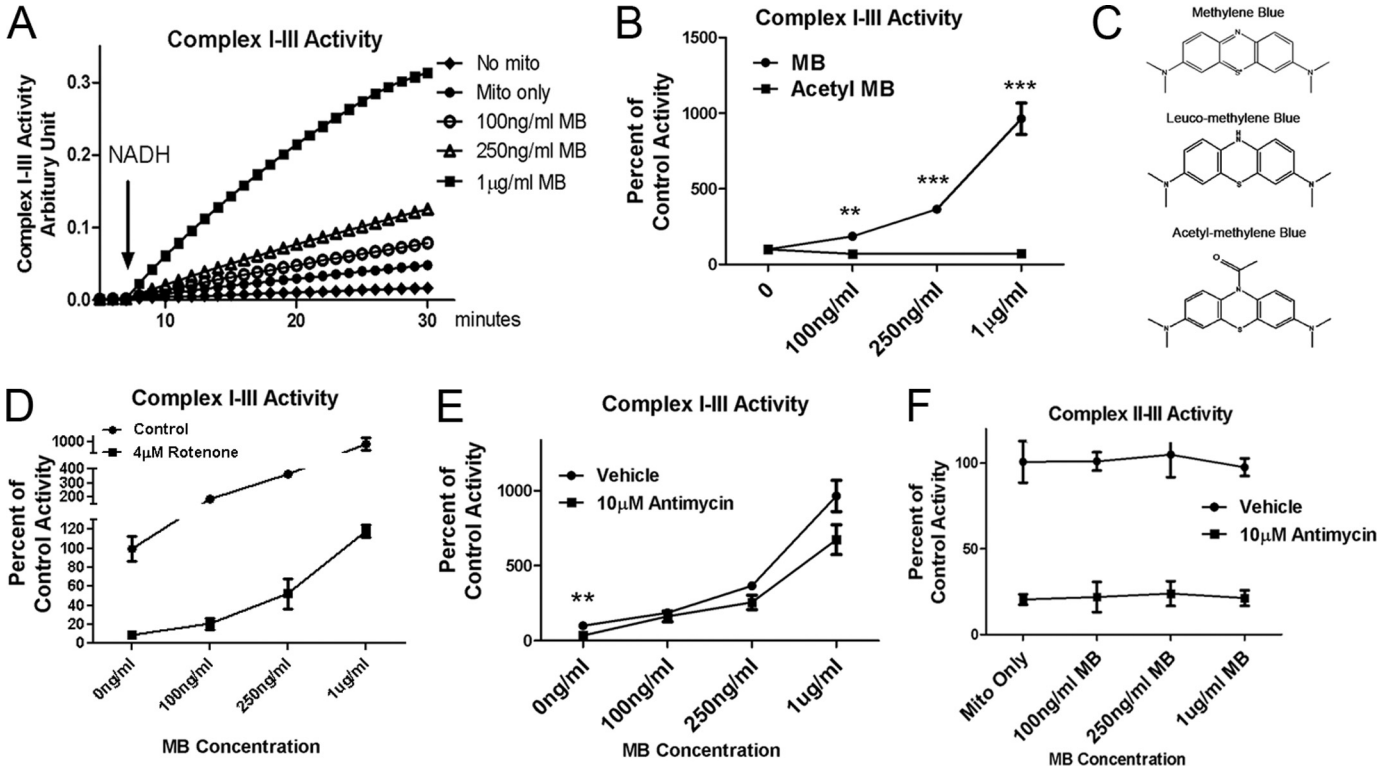

FIGURE 2. **Dose-dependent effects of MB in mitochondrial complex I-III and II-III activity in mitochondrial extracts.** *A*, representative assay of complex I-III activity; *B*, complex I-III activity with increasing dose of MB or acetyl MB, which is redox-disabled; *C*, chemical structure of MB, MBH_2, and acetyle MB. *D*, complex I-III activity with increasing dose of MB with/without the presence of complex I inhibitor (rotenone). *E*, complex I-III activity with increasing dose of MB with/without the presence of complex III inhibitor (antimycin A). *F*, complex II-III activity with increasing dose of MB with/without the presence of complex III inhibitor (antimycin A). *, **, and ***, significant difference from those without antimycin. *, $p < 0.05$; **, $p < 0.01$; ***, $p < 0.001$. *Error bars*, S.E.

MB, whereas 80.3 ± 9.6% cell survival was observed with MB at 10 ng/ml (26. 7 nM). A complete protection was found for MB at 100 ng/ml (267 nM) (Fig. 4*B*).

We further examined whether MB could function as a direct ROS scavenger. Glucose oxidase chronically oxidizes glucose in the medium to release H_2O_2, which results in cell death. MB failed to protect cells with such H_2O_2-induced oxidative damage (Fig. 4*C*). In contrast to these results with H_2O_2, MB (100 ng/ml) almost completely blocked the increase in mitochondrial superoxide (*Mitosox*) and total cellular ROS (*DCFH2*) production when rotenone was used to induce mitochondrial specific superoxide and ROS production in HT-22 cells (Fig. 4, *D* and *E*). Unlike many other antioxidants, MB is not an ROS scavenger; rather, it decreases the production of ROS by improving mitochondrial function.

MB Attenuates Neurological and Behavioral Deficit in a Rat Model of PD—We used systemic rotenone infusion to produce a rat model of PD. The effects of MB in this model were determined by neurological and behavioral assessment, biochemical analysis, and neuropathological evaluation. Rats treated with rotenone endured significant weight loss, which was attenuated by MB treatments (Fig. 5*A*). Significant locomotor deficits were found in rotenone-treated rats (Fig. 5*B*). In rotarod tests, control rats receiving vehicle showed improved performance in early sessions. In contrast, the rotenone-treated group showed decreased performance from the beginning of the sessions (5th day after rotenone infusion) and had lower performance throughout the sessions. MB treatment almost completely prevented these rotenone-induced locomotor deficits (Fig. 5*B*). In randomized blinded neurological assessment, significant deficits in all categories were observed in rotenone-treated animals, evidenced by the higher score at each assessment. MB treatment significantly improved all neurological scores in rotenone-treated rats (Fig. 5*C*).

Catalepsy was tested by measuring the descent latency after 5 days of rotenone infusion, using both bar and grid tests. In both tests, rotenone-treated animals showed marked deficiency, which was significantly improved by MB treatment. Specifically, rotenone prolonged descent latency in the bar test as compared with control animals, and MB treatment completely reversed such change induced by rotenone (Fig. 5*D*). Similarly, in the grid test, rotenone significantly decreased latency to fall, which was attenuated by MB treatment (Fig. 5*E*). In gait analysis, rotenone significantly decreased stride length, which was improved by MB treatment (Fig. 5*F*).

MB Rescues Rotenone-induced Dopamine Depletion, Mitochondrial Complex I-III Dysfunction, and ROS Overproduction in Vivo—We analyzed the levels of dopamine, dopamine metabolites, and 5-HT in striatum. Dopamine levels (Fig. 6*A*) as well as levels of its metabolite, 3,4-dihydroxyphenylacetic acid (DOPAC) (Fig. 6*B*), significantly decreased in striatum derived from the rotenone-treated group (ROT/Sal) compared with the control group (Veh/Sal). Consistently, such dopamine depletion was almost completely rescued by MB treatment (Fig. 6, *A* and *B*). Interestingly, there was no significant difference in 5-HT levels among all three groups of animals (data not

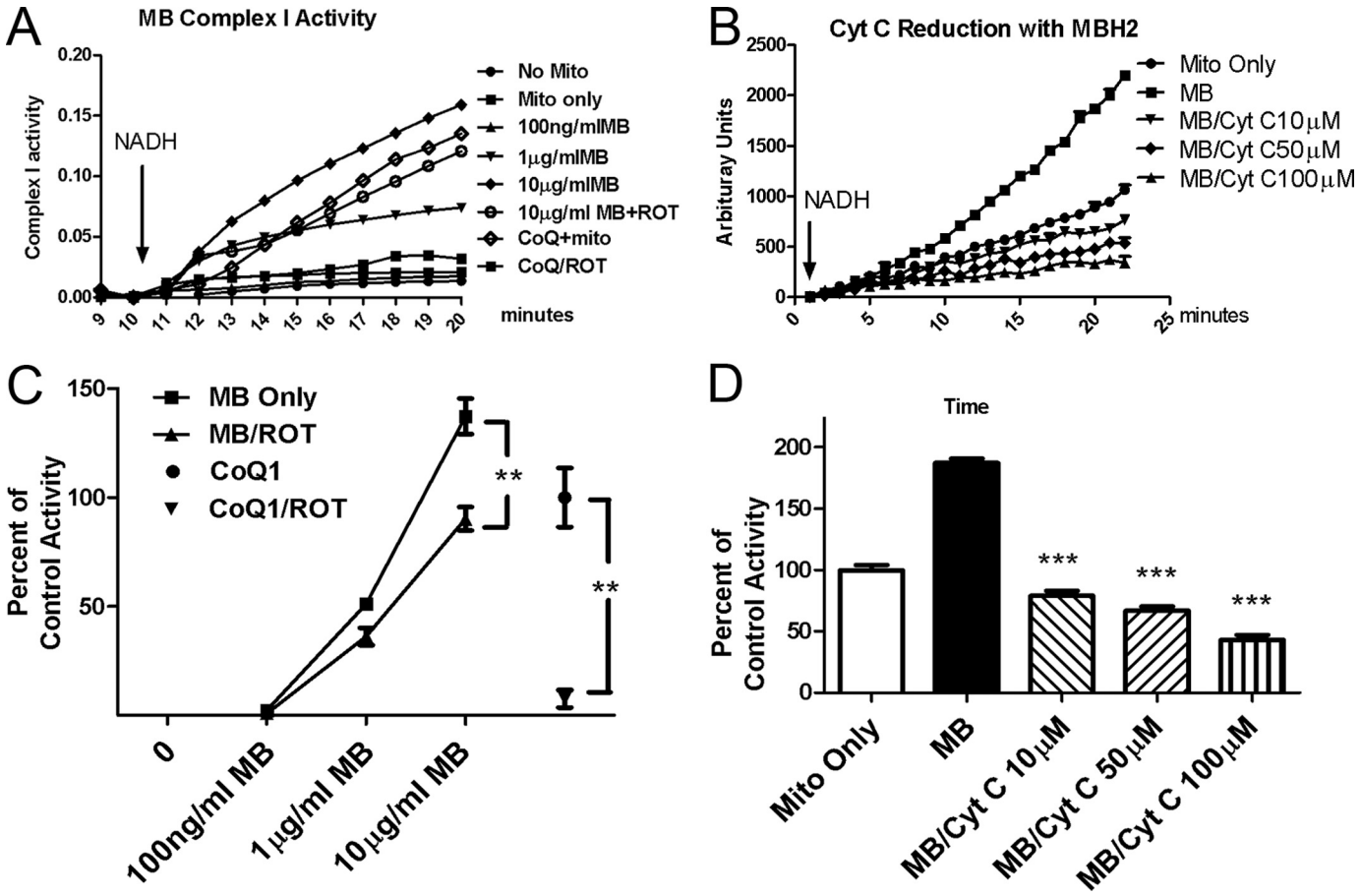

FIGURE 3. **MB forms a redox cycle between complex I and III.** *A* and *C*, MB is a complex I substrate accepting electrons from NADH in a dose-dependent manner and is insensitive to rotenone inhibition. Activity with coenzyme Q1 was used as 100% control. **, significant difference between the indicated groups. *B* and *D*, reduced MB donates electrons to oxidized cyt *c* in a dose-dependent manner. ***, significant difference from the MB-only group. *ROT*, rotenone; *CoQ1*, coenzyme Q1. *Top panels*, representative assays (A and *B*). *Bottom panels*, quantitative analysis of the corresponding assay (*C* and *D*). *Error bars*, S.E.

shown). These results confirmed the selective toxicity in the dopaminergic system induced by rotenone. We also assayed the mitochondrial activity in the brain extracts. A significant decrease of complex I-III activity was found in the ROT/Sal group, which was prevented by MB treatment (Fig. 6*C*). We interpret this as the result of ROS-induced complex I/III damage because previous publications suggested that complex I/III is the most sensitive component in the oxidative phosphorylation chain during stress (17, 18). We also measured overall ROS in the brain extracts and found that the ROT/Sal group had a significantly higher level of ROS compared with control groups. The increase of ROS by rotenone was also attenuated in the ROT/MB group (Fig. 6*D*).

MB Attenuates Dopaminergic Neuron Degeneration Induced by Chronic Rotenone Infusion—We used histological analysis for classical PD pathology. In the ROT/Sal group, inhibition of complex I resulted in degeneration of nigrostriatal dopaminergic neurons (Fig. 7). With this dose and duration of rotenone exposure, animals demonstrated severe loss of dopaminergic neuron at the substantia nigra pars compacta, together with varying degrees of striatal dopaminergic denervation (data not shown). Animals with dopaminergic neuron degeneration in substantia nigra were variable and correlate to their individual behavioral performance. Nearly complete loss of TH-positive cells in substantia nigra was observed in 5 of 11 rotenone-treated animals with the remaining showing varying degrees of loss of TH-positive cells. Furthermore, TH staining of the ventral tegmental area (VTA) showed remarkable nerve fiber degeneration in ROT/Sal-treated animals, a similar finding as observed previously (2). On the other hand, in the ROT/MB animals, a sufficient amount of TH-positive cell and nerve fiber was observed in SNC and VTA, respectively (Fig. 7). In addition, ubiquitin-positive cytoplasmic inclusions were observed in rats with dopaminergic neuron degeneration. Such inclusions were frequently clustered in the cytoplasm of ubiquitin-positive cells, similar to those seen in Lewy bodies. In our study, 6 of 11 ROT/Sal rats showed ubiquitin-positive aggregates, whereas such inclusion bodies were not found in any of the animals in the control group or the ROT/MB groups (Fig. 7).

To confirm that the loss of TH staining in dopaminergic neurons and nerve terminals was due to neurodegeneration, fluoro-jade B histochemistry was performed in brain sections from these animals. Fluoro-jade B-positive TH neurons were not found in either Veh/Sal group or the ROT/MB group. In contrast, fluoro-jade B-positive neurons were observed in the substantia nigra areas in 4 of 11 ROT/Sal animals (Fig. 8). We further examined the fluoro-jade B positive cells with double labeling of TH (Fig. 8). Almost all fluoro-jade B positive cells were TH-positive neurons. Together, double labeling of TH and fluoro-jade B conclusively demonstrated selective degen-

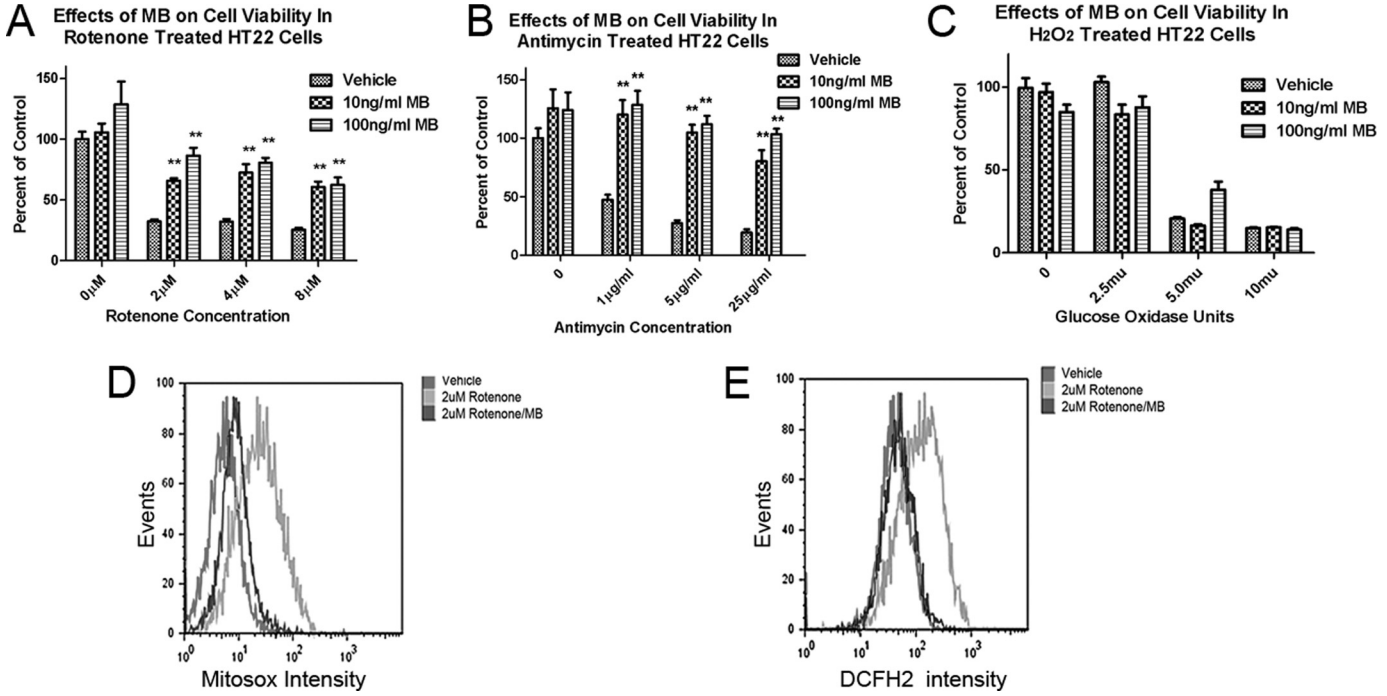

FIGURE 4. **Effects of MB in rotenone- and antimycin A-induced mitochondrial dysfunction and cell death.** *A* and *B*, neuroprotective effect of MB on rotenone-induced (*A*) and antimycin A-induced (*B*) cytotoxicity in HT22 cells. **, significant difference from vehicle. *C*, MB has no protection against H_2O_2 (released by glucose oxidase)-induced cytotoxicity. *D* and *E*, effects of MB on rotenone induced mitochondrial specific superoxide (*D*) and total cellular ROS (*E*). The *y axis* depicts the event (cell number in count $\times 10^3$), and the *x axis* depicts fluorescent intensity. Shown is the representative result from three independent sets of experiments. *Error bars*, S.E.

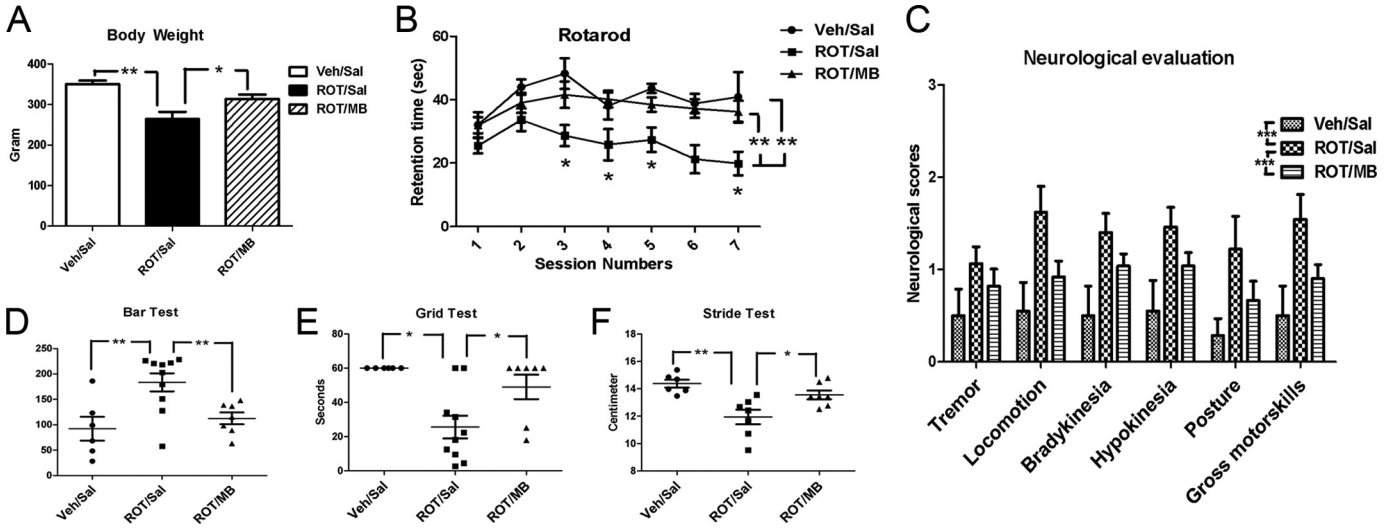

FIGURE 5. **Effects of MB on rotenone-induced neurological and behavioral deficit in rats.** *A*, MB prevents rat body weight loss induced by rotenone treatment. *B*, MB improved coordinated motor function deficiency induced by chronic rotenone treatment. **, significant difference between the indicated groups ($p < 0.01$). An *asterisk* in the individual sessions indicates that there is significant difference between ROT/Sal and both of the other two groups ($p < 0.05$). *C*, effects of MB on randomized blinded neurological assessments. ***, significant difference between the indicated groups ($p < 0.001$). *D* and *E*, effects of MB on catalepsy measurements in rotenone- and MB-treated rats with the bar test (*D*) and grid test (*E*). *F*, effects of MB on stride length in rotenone- and MB-treated rats in the gait test. *ROT*, rotenone-treated; *Sal*, saline (vehicle for MB); *Veh*, vehicle for rotenone. * and **, significant difference between the indicated groups in *D–F*. *Error bars*, S.E.

eration of nigra-striatal dopaminergic neurons in rotenone-infused animals, which was almost completely blocked by MB.

MB Reduces Cerebral Ischemia Reperfusion Damage Induced by Transient Focal Cerebral Ischemia—We assessed the neuroprotective action of MB in an ischemic stroke model of transient middle cerebral artery occlusion in rats. Massive mitochondrial failure, indicated by reduced ETC complex I, III, and IV activities was observed at 24 h after cerebral ischemia/reperfusion injury (Fig. 9*A*). By rerouting electron transfer, which bypasses complex I and III blockage, a single dosage of MB at 500 μg/kg significantly reduced the ischemic lesion volume (Fig. 9, *B* and *C*).

DISCUSSION

Neuroprotection is a therapeutic approach that aims to prevent or attenuate neuronal degeneration and loss of function in

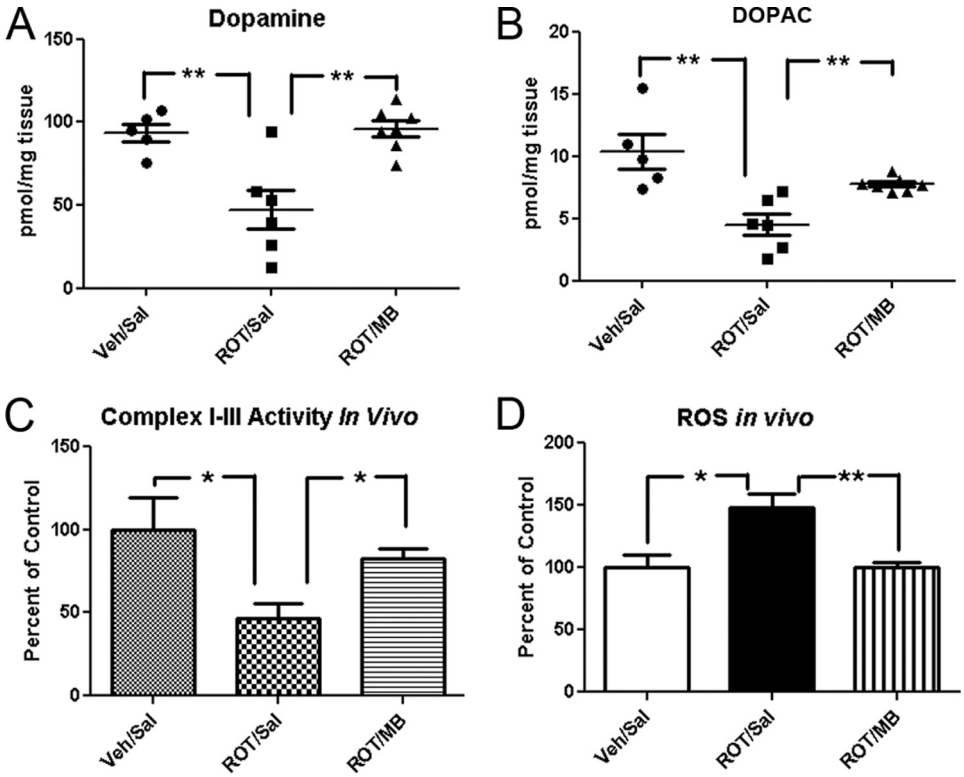

FIGURE 6. **Effects of MB and rotenone on dopamine and DOPAC levels, mitochondrial complex I-III activity, and total ROS *in vivo*.** *A* and *B*, effects of rotenone and MB treatment on striatum dopamine (*A*) and DOPAC (*B*) levels. *C* and *D*, mitochondrial I-III activity (*C*) and total ROS (*D*) in rotenone- and MB-treated rats. All numbers were normalized to percentage of control groups. * and **, significant difference between the indicated groups in all *panels*. *Error bars*, S.E.

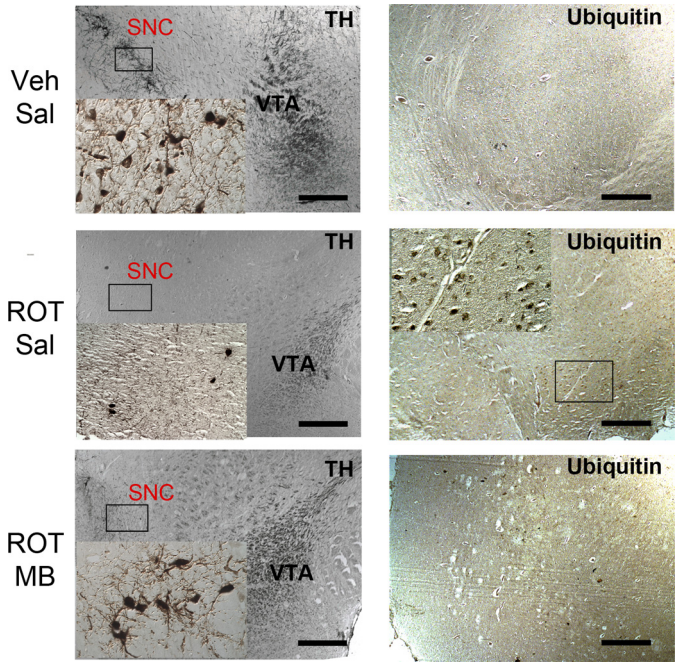

FIGURE 7. **Effects of MB on rotenone-induced nigrostriatal dopaminergic neurodegeneration.** Coronal brain sections from control (*Veh/Sal*), rotenone-treated (*ROT/Sal*), and rotenone/MB-treated (*ROT/MB*) rats were immunostained for TH (*left*) and ubiquitin (*right*). TH immunohistochemistry was shown at low magnification and high magnification in the SNC region. Dopaminergic denervation, cell body shrinkage, and neuronal loss were clearly observed in the ROT/Sal group, and all were improved in the MB treatment group. Dopaminergic fibers were sparse in VTA in the ROT/Sal group and improved in the ROT/MB group. Neurons with positive ubiquitin immunostaining were observed only in the ROT/Sal group. *Scale bars*, 200 μm.

neurological diseases. Neuroprotective strategies, including but not limited to free radical scavengers, ion channel modulators, and anti-inflammatory agents, have been extensively explored in the last 2 decades (19). Unfortunately, despite promising results from preclinical studies, outcomes of clinical neuroprotection trials have been repeatedly disappointing (8, 20). Increasing evidence has indicated that mitochondrial dysfunction is a common pathological mechanism that underlines many neuropathological conditions. Endogenous ETC component supplementation, such as with coenzyme Q10, was explored for their neuroprotective effects (21, 22). In addition, other identified neuroprotectants, such as estrogen, have been found to increase gene expression for many key components of the ETC complexes (23). However, the consistent failure of all of these approaches has cast doubt on the current neuroprotective strategies. In the present study, we identified alternative mitochondrial electron transfer as a novel neuroprotective strategy. The alternative electron transfer through MB redox cycle bypasses the inhibition of ETC complex I and III and avoids overproduction of free radical, hence providing neuroprotection in both chronic and acute neurological diseases.

Current evidence suggests that it is not the mitochondrial energy defect *per se* but rather the overproduction of ROS induced by blockage of mitochondrial complexes that accounts for the neurodegeneration in many neuropathological conditions (24–26). In fact, cells can survive via many alternative mechanisms other than mitochondrial oxidative phosphorylation, such as anaerobic glycolysis and autophagy. In our observation, complex IV (KCN) or complex V (oligomycin) inhi-

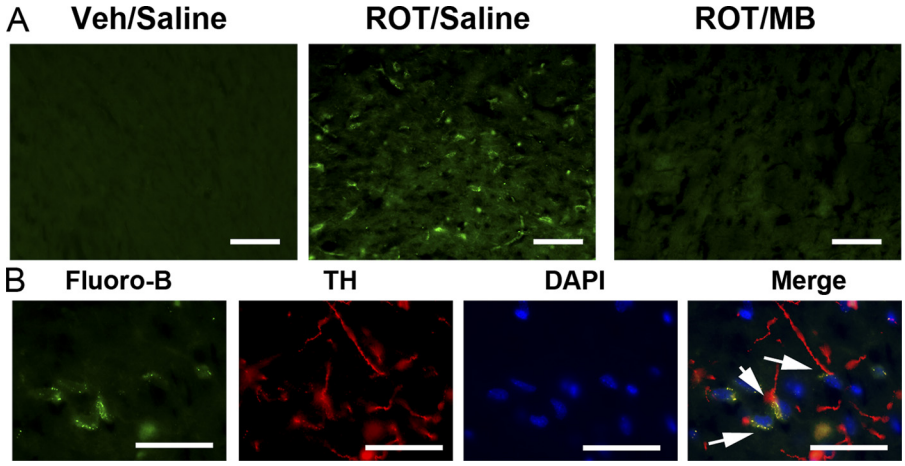

FIGURE 8. **MB attenuates rotenone induced fluoro-jade B-labeled neurodegeneration in TH-positive dopaminergic neurons.** *A*, many degenerated cell bodies of nigrostriatal dopaminergic neurons were positively labeled by fluoro-jade B in the SNC area in ROT/Sal animals. *B*, nigral neurons were double labeled with fluoro-Jade B and TH, showing that these were degenerating dopaminergic neurons in SNC. The *arrowheads* indicate the presence of double labeled neurons with both TH and fluoro-jade B. Such fluoro-jade B-positive neurons were identified in half of the ROT/Sal group that had severe neuronal loss and behavioral deficiency. No fluoro-jade B-positive neurons were detected in Veh/Sal or ROT/MB groups. *Scale bar*, 100 μm (*A*) and 50 μm (*B*).

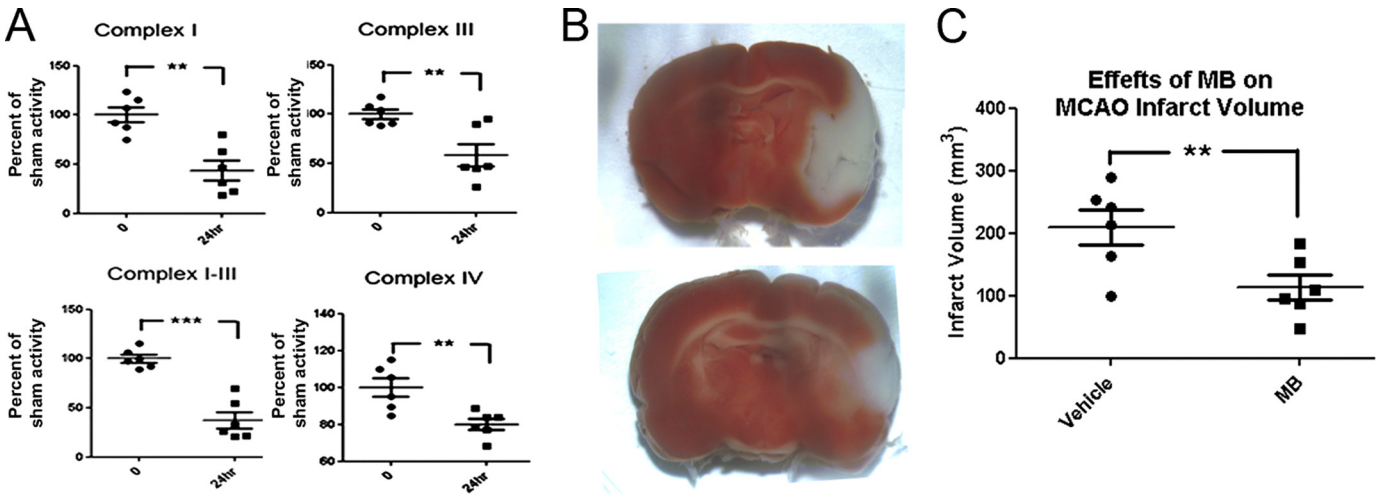

FIGURE 9. **MB reduces cerebral ischemia reperfusion damage induced by transient focal cerebral ischemia.** *A*, ischemia/reperfusion injury, induced by 1 h of middle cerebral artery occlusion and 24 h of reperfusion, inhibits mitochondrial complex activities (*I*, *III*, *I-III*, and *IV*). *B*, ischemic lesion depicted by triphenyltetrazolium chloride staining (*white area*) in the representative brain sections from control-treated (*top*) and MB-treated (*bottom*) rats at 24 h after ischemic stroke. *C*, quantification of ischemic lesion volume with vehicle or MB treatment. All data are represented as mean ± S.E. *, $p < 0.05$; **, $p < 0.01$; ***, $p < 0.001$.

bition reduces cell growth but does not convey direct cytotoxicity. Previous studies indicate that neither complex IV nor complex V is involved in electron leakage and ROS production (27, 28). We found that inhibition of complex IV or V induced anaerobic glycolytic activity and lactate production, which compensated for the decrease of ATP production (data not shown). On the other hand, complex I/III blockage directly cause the leakage of electrons, which react oxygen molecules, lead to ROS generation, and induce cytotoxicity. Thus, an alternative electron transfer pathway can bypass complex I/III blockage, avoid ROS production, and provide neuroprotection.

MB has a very low redox potential of 11 mV and is very efficient cycling between oxidized and reduced forms (10). In the current study, we determined the action of MB in ETC complex activities. Our results demonstrated that MB functions as an alternative electron carrier similar to the endogenous coenzyme Qs in mitochondrial ETC. On the other hand, MB-mediated electron transfer is insensitive to either rotenone or antimycin A inhibition, suggesting that MB provides an alternative route for electron transfer. Upon the completion of the redox cycle (MB $\rightarrow$ MBH_2 $\rightarrow$ MB), electrons from NADH are delivered to cyt *c* in an alternate route that is insensitive to complex I and III blockage. Such a mechanism is further confirmed by a *de novo* synthesized MB derivative with the disabled redox center by *N*-acetylation. Acetyl-MB completely lost its ability to enhance electron transfer between complex I and III. The alternative electron transfer through MB prevents the "electron leakage" induced by complex I/III inhibition and avoids the massive ROS production during complex I/III inhibition (Fig. 10).

In cell cultures, MB provides protection against mitochondrial inhibition-induced ROS overproduction, mitochondrial dysfunction, and cytotoxicity. Given the high enzymatic efficacy and potency, the alternative electron transfer strategy requires much lower concentrations for neuroprotection as compared with the traditional free radical scavengers. Consistently, the neuropro-

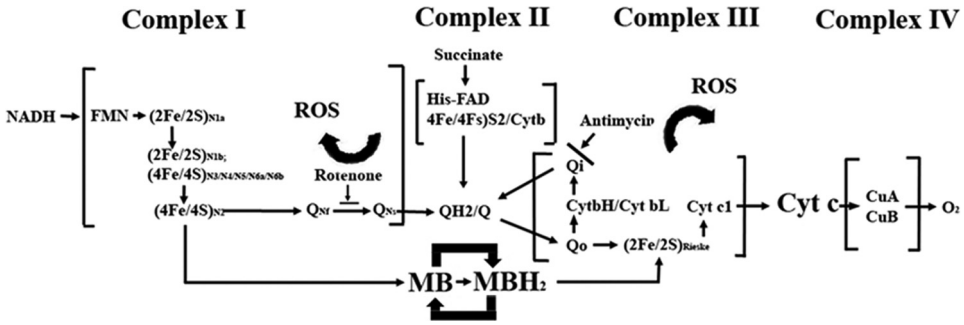

FIGURE 10. **Illustrations of the proposed mechanism by which MB facilitates electron transfers in the oxidative phosphorylation chain in the presence of rotenone and antimycin A inhibition.**

tective effects of MB occur at very low concentrations with an EC_{50} of 0.1762 nM against glutamate toxicity in HT22 cells. Therefore, the alternative electron transfer strategy is fundamentally different from traditional free radical scavenger approach. Rather, it avoids the production of ROS by rerouting electron transfer and bypasses complex I/III inhibition. Indeed, MB failed to provide protection against direct hydrogen peroxide insult even with much higher concentrations.

We further determined the effects of this novel neuroprotective strategy in animal models of PD and ischemic stroke. From both epidemiological (29) and basic research (2, 30), growing evidence has indicated that complex I dysfunction is the primary factor in PD pathogenesis. It has been known that complex I activity is deficient in the brain as well as peripheral tissues in PD patients (reviewed in Refs. 24, 26, 31, and 32). Such concepts are further proved by the recently developed rotenone PD model (2, 33). Many features of PD have been observed in the systemic rotenone model, including complex I impairment (2), oxidative damage (34), accumulation and aggregation of α-synuclein in select dopaminergic neurons, and impairment of nigral ubiquitin-proteasome system function with accumulation of polyubiquitinated proteins (2). Moreover, two genetic causes of PD, mutations in Parkin and PINK1, have been associated with defective complex I activity (1, 35). Consistently, overexpression of NDI1, a yeast gene encoding a single subunit rotenone-insensitive NADH-quinone oxidoreductase, in rodents could prevent respiratory deficiencies and attenuate Parkinson-like symptoms in animals treated with rotenone or MPTP (36). Our *in vivo* studies indicated that MB attenuates complex I inhibition-induced neurodegeneration in dopaminergic neurons and provides protection against rotenone-induced Parkinson-like behavioral, neurochemical, and neuropathological features.

The role of ROS in the pathogenesis of cerebral ischemia reperfusion injury is well known. Reperfusion produces a burst in ROS formation after cerebral ischemia and has been known as one of the major mechanisms by which reperfusion worsens ischemic damage (37). Antioxidant has been viewed as one of the most promising neuroprotective strategies for the treatment of ischemic stroke. However, the failure of the SAINT II trial has raised concerns regarding the traditional free radical trapping strategy (38). Instead of neutralizing the free radical, the alternative electron transfer strategy blocked the overproduction of ROS generated by the inhibition of ETC complex I and III. In addition, our study demonstrated that MB increases the oxygen consumption rate and decreases the extracellular acidification rate, which could potentially prevent the superoxide production derived from the excessive oxygen supply during the reperfusion. Consistently, our *in vivo* study demonstrated that MB, as an alternative electron carrier, significantly decreased the cerebral ischemia reperfusion damage induced by transient focal cerebral ischemia.

There are other considerations for the role of alternative electron transfer in mitochondrial functions. The mitochondrial ETC removes electrons from an electron donor (NADH or $FADH_2$) and passes them to a terminal electron acceptor (O_2) via a series of redox reactions. These reactions are coupled to the creation of a proton gradient across the mitochondrial inner membrane, which functions as the direct driving force for ATP synthesis. In ETC, complexes I, III, and IV function as the proton pumps. An alternate route to ETC could bypass the proton pump function in these complexes and might reduce the efficiency of ATP production. However, our study demonstrated that MB could enhance ATP production, suggesting that MB does not comprise the function of complexes I, III, and IV as proton pumps.

In addition to the capacity as an alternative electron carrier, many other functions of MB have previously been described. It was shown that MB can delay senescence and extend the life span of human IMR90 fibroblasts in tissue culture (10). It has also been indicated that MB can penetrate the blood brain barrier, increase cyt *c* oxidase (complex IV) activity, improve cognitive function in rats (39), and protect against methylmalonate-induced seizures (40). As a century-old drug, MB has been in medical use for many years in various pathological conditions (41, 42). The therapeutic potential of MB has been demonstrated clinically against many diseases, including endotoxin-induced lung injury, bacterial lipopolysaccharide-induced fever (43–45), cyclosporin-induced kidney injury (46), doxorubicin-induced heart injury (47), and pancreas injury induced by streptozotocin (48). Recently, MB was reported to attenuate Tau aggregation, and it is currently in phase II clinical trials for treatment of Alzheimer disease. Many other activities have also been demonstrated with MB, including inhibition of nitric-oxide synthase (49, 50) and monoamine oxidase A (51), which may also contribute to the illustrated neuroprotective action. However, some of these functions might be secondary to the currently described mitochondrial mechanism and warrant further investigation.

In summary, we have identified a novel neuroprotective strategy represented by MB in the present study. We have demonstrated that MB could function as an electron carrier and provide an alternative electron transfer along ETC, avoid ROS overproduction induced by ETC blockage, and maintain mitochondrial function. We have tested this novel neuroprotective strategy in two animal models of neurological diseases. In an animal model of Parkinsonism, MB was able to attenuate rotenone-induced motor deficits and nigral-dopaminergic neuronal degeneration. In an ischemic stroke model, MB significantly reduced cerebral ischemia reperfusion damage. Considering that MB has been in clinical use for over a century with few known side effects, the identified novel neuroprotective strategy of alternative electron transfer is now ready for testing in clinical settings and might lead to the discovery of promising treatments for the mitochondria dysfunction-related neurological diseases, such as PD and stroke.

REFERENCES

1. Liu, W., Vives-Bauza, C., Acín-Peréz, R., Yamamoto, A., Tan, Y., Li, Y., Magrané, J., Stavarache, M. A., Shaffer, S., Chang, S., Kaplitt, M. G., Huang, X. Y., Beal, M. F., Manfredi, G., and Li, C. (2009) *PloS One* **4,** e4597
2. Betarbet, R., Sherer, T. B., MacKenzie, G., Garcia-Osuna, M., Panov, A. V., and Greenamyre, J. T. (2000) *Nat. Neurosci.* **3,** 1301–1306
3. Yao, J., Irwin, R. W., Zhao, L., Nilsen, J., Hamilton, R. T., and Brinton, R. D. (2009) *Proc. Natl. Acad. Sci. U.S.A.* **106,** 14670–14675
4. Vosler, P. S., Graham, S. H., Wechsler, L. R., and Chen, J. (2009) *Stroke* **40,** 3149–3155
5. Wallace, D. C. (2005) *Annu. Rev. Genet.* **39,** 359–407
6. Chaturvedi, R. K., and Beal, M. F. (2008) *Ann. N.Y. Acad. Sci.* **1147,** 395–412
7. Galluzzi, L., Blomgren, K., and Kroemer, G. (2009) *Nat. Rev. Neurosci.* **10,** 481–494
8. O'Collins, V. E., Macleod, M. R., Donnan, G. A., Horky, L. L., van der Worp, B. H., and Howells, D. W. (2006) *Ann. Neurol.* **59,** 467–477
9. Olanow, C. W., Kieburtz, K., and Schapira, A. H. (2008) *Ann. Neurol.* **64,** Suppl. 2, S101–S110
10. Atamna, H., Nguyen, A., Schultz, C., Boyle, K., Newberry, J., Kato, H., and Ames, B. N. (2008) *FASEB J.* **22,** 703–712
11. Tokumitsu, Y., and Ui, M. (1973) *Biochim. Biophys. Acta* **292,** 310–324
12. Trounce, I. A., Kim, Y. L., Jun, A. S., and Wallace, D. C. (1996) *Methods Enzymol.* **264,** 484–509
13. Lenaz, G., Fato, R., Baracca, A., and Genova, M. L. (2004) *Methods Enzymol.* **382,** 3–20
14. Klintenberg, R., Arts, J., Jongsma, M., Wikström, H., Gunne, L., and Andrén, P. E. (2003) *Eur. J. Pharmacol.* **459,** 231–237
15. Liu, D. Z., Zhu, J., Jin, D. Z., Zhang, L. M., Ji, X. Q., Ye, Y., Tang, C. P., and Zhu, X. Z. (2007) *J. Ethnopharmacol.* **112,** 327–332
16. Srinivasan, J., and Schmidt, W. J. (2004) *Behav. Brain Res.* **151,** 191–199
17. Rouslin, W. (1983) *Am. J. Physiol.* **244,** H743–H748
18. Chen, Q., Moghaddas, S., Hoppel, C. L., and Lesnefsky, E. J. (2008) *Am. J. Physiol. Cell Physiol.* **294,** C460–C466
19. Ginsberg, M. D. (2008) *Neuropharmacology* **55,** 363–389
20. Löhle, M., and Reichmann, H. (2010) *J. Neurol. Sci.* **289,** 104–114
21. Storch, A., Jost, W. H., Vieregge, P., Spiegel, J., Greulich, W., Durner, J., Müller, T., Kupsch, A., Henningsen, H., Oertel, W. H., Fuchs, G., Kuhn, W., Niklowitz, P., Koch, R., Herting, B., and Reichmann, H. (2007) *Arch. Neurol.* **64,** 938–944
22. Yang, L., Calingasan, N. Y., Wille, E. J., Cormier, K., Smith, K., Ferrante, R. J., and Beal, M. F. (2009) *J. Neurochem.* **109,** 1427–1439
23. O'Lone, R., Knorr, K., Jaffe, I. Z., Schaffer, M. E., Martini, P. G., Karas, R. H., Bienkowska, J., Mendelsohn, M. E., and Hansen, U. (2007) *Mol. Endocrinol.* **21,** 1281–1296
24. Fukui, H., and Moraes, C. T. (2008) *Trends Neurosci.* **31,** 251–256
25. Cassarino, D. S., Fall, C. P., Swerdlow, R. H., Smith, T. S., Halvorsen, E. M., Miller, S. W., Parks, J. P., Parker, W. D., Jr., and Bennett, J. P., Jr. (1997) *Biochim. Biophys. Acta* **1362,** 77–86
26. Gandhi, S., and Wood, N. W. (2005) *Hum. Mol. Genet.* **14,** 2749–2755
27. Ladiges, W., Wanagat, J., Preston, B., Loeb, L., and Rabinovitch, P. (2010) *Aging Cell* **9,** 462–465
28. Ganguly, A., Basu, S., Chakraborty, P., Chatterjee, S., Sarkar, A., Chatterjee, M., and Choudhuri, S. K. (2010) *PloS One* **5,** e11253
29. Dhillon, A. S., Tarbutton, G. L., Levin, J. L., Plotkin, G. M., Lowry, L. K., Nalbone, J. T., and Shepherd, S. (2008) *J. Agromedicine* **13,** 37–48
30. Nicklas, W. J., Vyas, I., and Heikkila, R. E. (1985) *Life Sci.* **36,** 2503–2508
31. Mizuno, Y., Ohta, S., Tanaka, M., Takamiya, S., Suzuki, K., Sato, T., Oya, H., Ozawa, T., and Kagawa, Y. (1989) *Biochem. Biophys. Res. Commun.* **163,** 1450–1455
32. Haas, R. H., Nasirian, F., Nakano, K., Ward, D., Pay, M., Hill, R., and Shults, C. W. (1995) *Ann. Neurol.* **37,** 714–722
33. Greenamyre, J. T., MacKenzie, G., Peng, T. I., and Stephans, S. E. (1999) *Biochem. Soc. Symp.* **66,** 85–97
34. Testa, C. M., Sherer, T. B., and Greenamyre, J. T. (2005) *Mol. Brain Res.* **134,** 109–118
35. Müftüoglu, M., Elibol, B., Dalmizrak, O., Ercan, A., Kulaksiz, G., Ogüs, H., Dalkara, T., and Ozer, N. (2004) *Mov. Disord.* **19,** 544–548
36. Seo, B. B., Nakamaru-Ogiso, E., Flotte, T. R., Matsuno-Yagi, A., and Yagi, T. (2006) *J. Biol. Chem.* **281,** 14250–14255
37. Schaller, B., and Graf, R. (2004) *J Cereb. Blood Flow Metab.* **24,** 351–371
38. Diener, H. C., Lees, K. R., Lyden, P., Grotta, J., Davalos, A., Davis, S. M., Shuaib, A., Ashwood, T., Wasiewski, W., Alderfer, V., Hårdemark, H. G., and Rodichok, L. (2008) *Stroke* **39,** 1751–1758
39. Callaway, N. L., Riha, P. D., Bruchey, A. K., Munshi, Z., and Gonzalez-Lima, F. (2004) *Pharmacol. Biochem. Behav.* **77,** 175–181
40. Furian, A. F., Fighera, M. R., Oliveira, M. S., Ferreira, A. P., Fiorenza, N. G., de Carvalho Myskiw, J., Petry, J. C., Coelho, R. C., Mello, C. F., and Royes, L. F. (2007) *Neurochem. Int.* **50,** 164–171
41. Naylor, G. J., Martin, B., Hopwood, S. E., and Watson, Y. (1986) *Biol. Psychiatry* **21,** 915–920
42. Peer, G., Itzhakov, E., Wollman, Y., Chernihovsky, T., Grosskopf, I., Segev, D., Silverberg, D., Blum, M., Schwartz, D., and Iaina, A. (2001) *Nephrol. Dial. Transplant.* **16,** 1436–1441
43. Galili, Y., Kluger, Y., Mianski, Z., Iaina, A., Wollman, Y., Marmur, S., Soffer, D., Chernikovsky, T., Klausner, J. P., and Robau, M. Y. (1997) *Eur. Surg. Res.* **29,** 390–395
44. Demirbilek, S., Sizanli, E., Karadag, N., Karaman, A., Bayraktar, N., Turkmen, E., and Ersoy, M. O. (2006) *Eur. Surg. Res.* **38,** 35–41
45. Riedel, W., Lang, U., Oetjen, U., Schlapp, U., and Shibata, M. (2003) *Mol. Cell. Biochem.* **247,** 83–94
46. Rezzani, R., Rodella, L., Corsetti, G., and Bianchi, R. (2001) *Nephron* **89,** 329–336
47. Hrushesky, W. J., Olshefski, R., Wood, P., Meshnick, S., and Eaton, J. W. (1985) *Lancet* **1,** 565–567
48. Haluzik, M., Nedvídková, J., and Skrha, J. (1999) *Endocr. Res.* **25,** 163–171
49. Marczin, N., Ryan, U. S., and Catravas, J. D. (1992) *J. Pharmacol. Exp. Ther.* **263,** 170–179
50. Mayer, B., Brunner, F., and Schmidt, K. (1993) *Eur. Heart J.* **14,** Suppl. I, 22–26
51. Ramsay, R. R., Dunford, C., and Gillman, P. K. (2007) *Br. J. Pharmacol.* **152,** 946–951